

## Supplementary Materials

### **Versatile van der Waals Heterostructures of $\gamma$ -GeSe with h-BN/Graphene/MoS<sub>2</sub>**

Changmeng Huan<sup>1,2</sup>, Pu Wang<sup>1,2</sup>, Binghan He<sup>1,2</sup>, Yongqing Cai<sup>3\*</sup>, Qingqing Ke<sup>1,2\*</sup>

<sup>1</sup>School of Microelectronics Science and Technology, Sun Yat-sen university, Zhuhai 519082, China

<sup>2</sup>Guangdong Provincial Key Laboratory of Optoelectronic Information Processing Chips and Systems, Sun Yat-sen University, Zhuhai 519082, China

<sup>3</sup>Joint Key Laboratory of the Ministry of Education, Institute of Applied Physics and Materials Engineering, University of Macau, Taipa, Macau, China

\* Corresponding authors

E-mail: [yongqingcai@um.edu.mo](mailto:yongqingcai@um.edu.mo); [keqingq@mail.sysu.edu.cn](mailto:keqingq@mail.sysu.edu.cn)

## Lattice mismatches and strains

The lattice mismatches ( $\eta$ ) were calculated through

$$\eta = \left| \frac{a_0 \times n - a_v}{a_v} \right|$$

where  $a_0$  and  $a_v$  represent the lattice constant of the freestanding monolayers and the vdWHs, respectively,  $n$  represents the scaling factor from monolayer unit cells to heterojunction supercells.

Furthermore, the strains ( $\varepsilon$ ) induced by lattice mismatches can be calculated as

$$\varepsilon = \frac{a_v - a_0 \times n}{a_0 \times n}$$

The calculated lattice constants, lattice mismatches and strains are shown in the Table S1.

**Table S1.** The calculated lattice constants and lattice mismatches of  $\gamma$ -GeSe/BN,  $\gamma$ -GeSe/graphene, and  $\gamma$ -GeSe/MoS<sub>2</sub> vdWHs, and the strains of constituent layers in vdWHs relative to their freestanding monolayers where negative (positive) values represent compressive (tensile) strain.

	$\gamma$ -GeSe	BN	$\gamma$ -GeSe	Graphene	$\gamma$ -GeSe	MoS <sub>2</sub>
$a_0$ (Å)	3.76	2.51	3.76	2.47	3.76	3.15
$a_v$ (Å)	7.53		7.42		6.39	
$\eta$ (%)	0.13%	0	1.35%	0.13%	1.92%	1.41%
$\varepsilon$ (%)	+0.13%	0	-1.33%	+0.13%	-1.88%	+1.43%

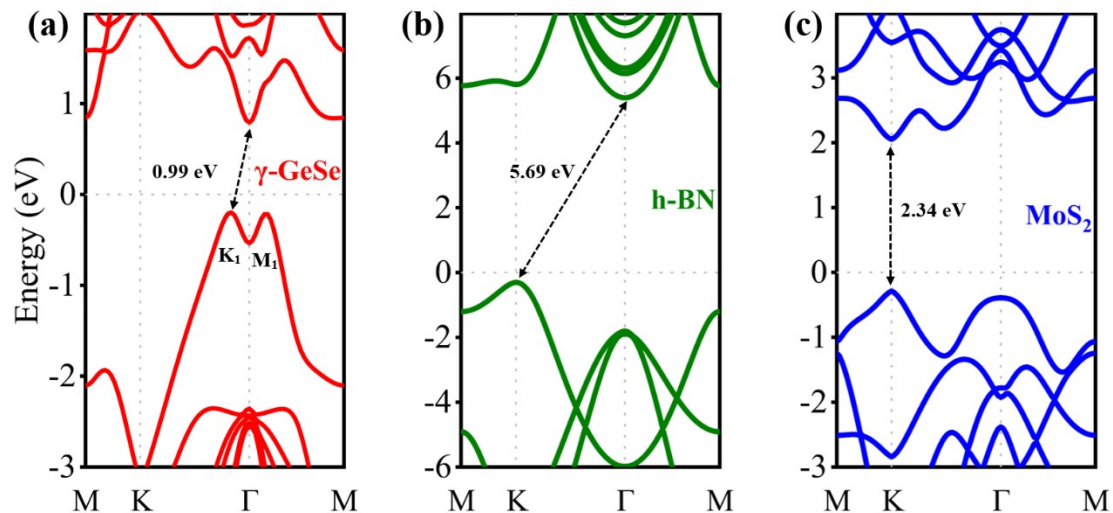


**Fig. S1** The band structures of  $\gamma$ -GeSe (a), h-BN (b), and 2H-MoS<sub>2</sub> (c) monolayers by HSE06 functionals. The Fermi level is aligned to 0 eV.

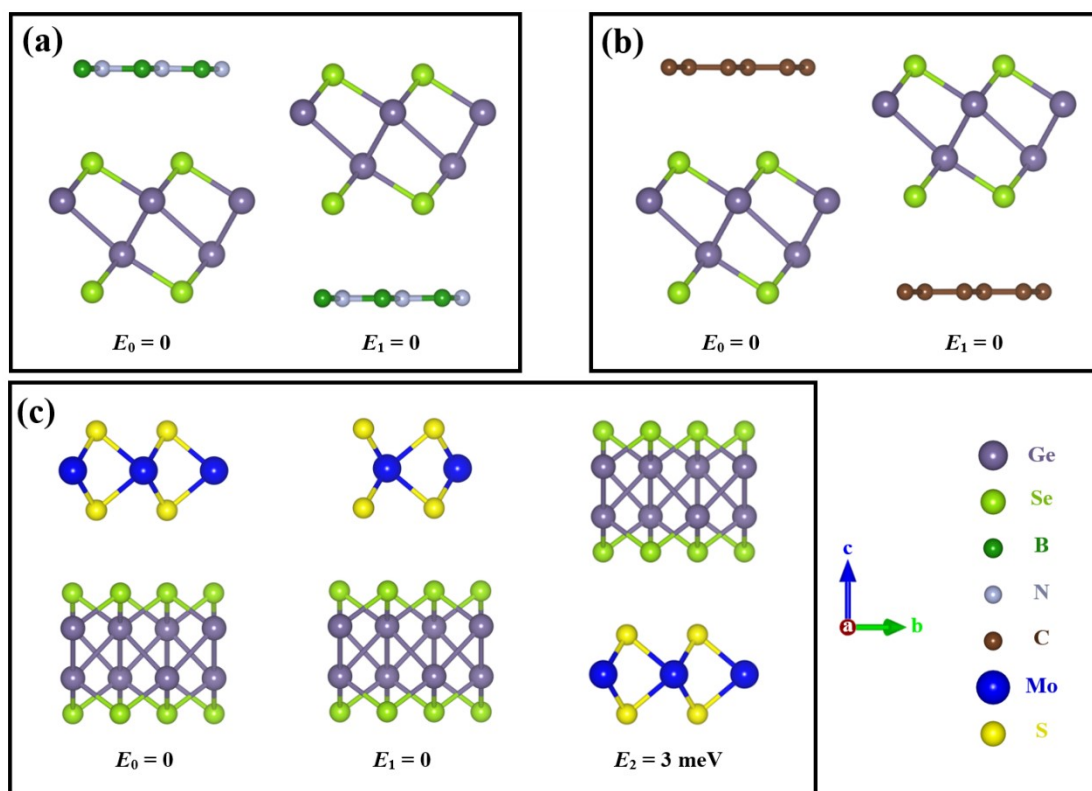


**Fig. S2** Total energies of  $\gamma$ -GeSe/BN (a),  $\gamma$ -GeSe/graphene (b), and  $\gamma$ -GeSe/MoS<sub>2</sub> (c) vdWHs with different stacking order. The energy of  $\gamma$ -GeSe/*X* vdWH ( $E_0$ ) discussed in this work is set to 0 for reference.

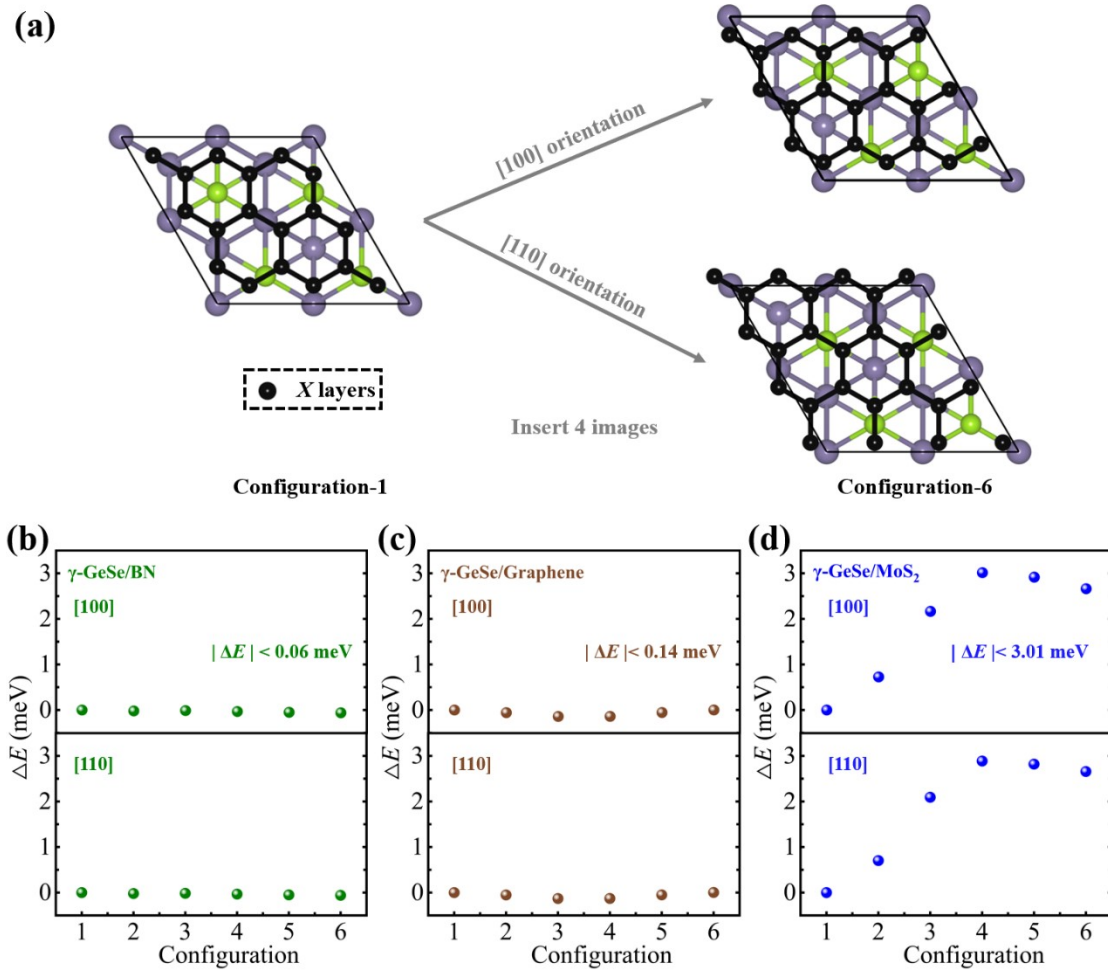


**Fig. S3** Schematic of the structures (a) obtained by linearly shifting half the unit-cell parameters along the [100] and [110] orientation, and the relative energies of the six structures of  $\gamma$ -GeSe/BN (b),  $\gamma$ -GeSe/graphene (c), and  $\gamma$ -GeSe/MoS<sub>2</sub> vdWHs (d). The total energy of configuration-1 is set to 0 as a reference.

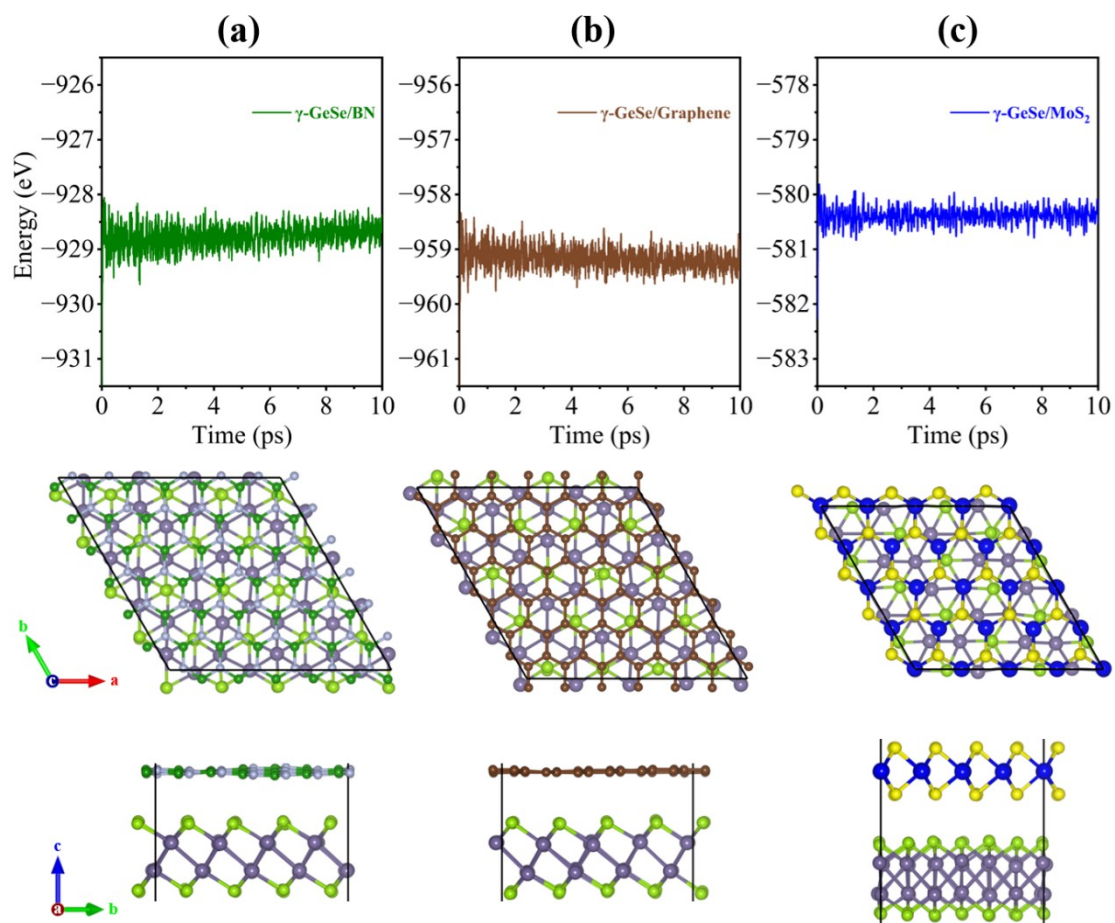


**Fig. S4** Total energy evolution and 10 ps snapshots of  $\gamma$ -GeSe/BN (a),  $\gamma$ -GeSe/graphene (b), and  $\gamma$ -GeSe/MoS<sub>2</sub> (c) vdWHs from ab initio molecular dynamics calculations (AIMD).

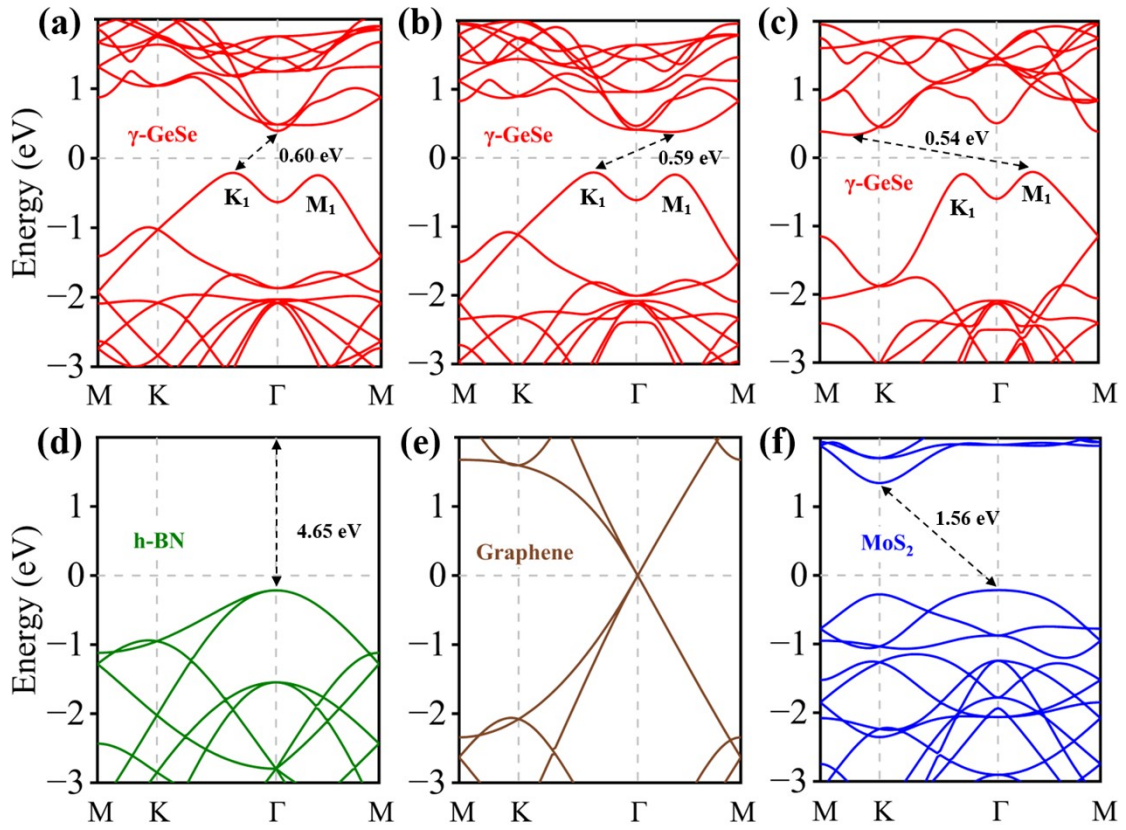


**Fig. S5** Band structures of (a)  $\gamma$ -GeSe and (d) h-BN monolayer supercell under the strain equivalent to that in the  $\gamma$ -GeSe/BN vdWH, band structures of (b)  $\gamma$ -GeSe and (e) graphene monolayer supercell under the strain equivalent to that in the  $\gamma$ -GeSe/graphene vdWH, and (c)  $\gamma$ -GeSe and (f) MoS<sub>2</sub> monolayer supercell under the strain equivalent to that in  $\gamma$ -GeSe/MoS<sub>2</sub> vdWH.

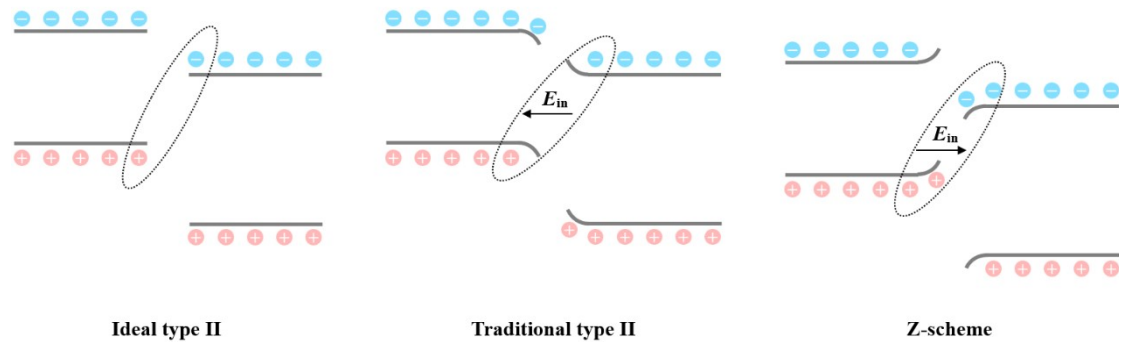


**Fig. S6** Band alignment interface of ideal type II, traditional type I, and Z-scheme.

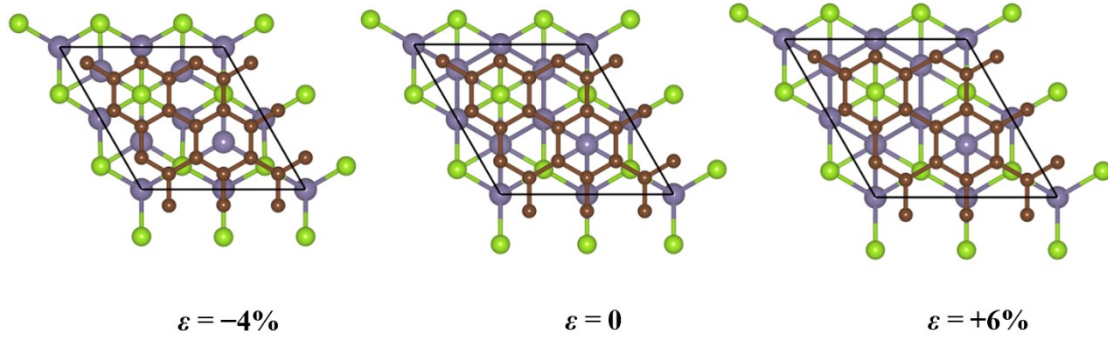


**Fig. S7** Top view of the optimized heterostructures of  $\gamma$ -GeSe/graphene under different strains.

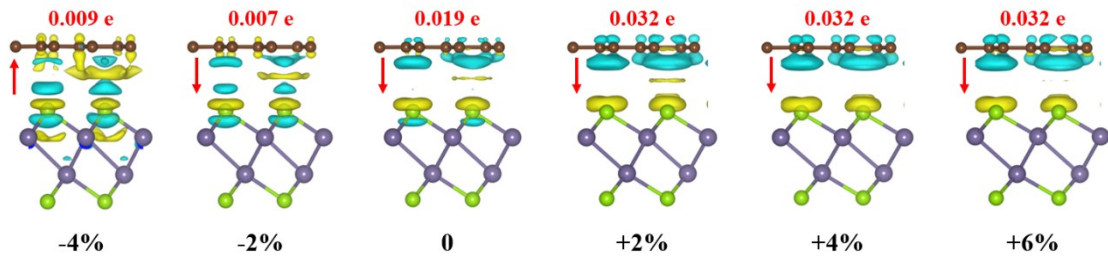


**Fig. S8** Front view of the DCD isosurface for  $\gamma$ -GeSe/graphene vdWH under different strains with the isovalue of  $10^{-4} e/\text{\AA}^3$ . The red arrows and numerical values indicate the direction and amount of charge transfer, respectively.

### Discussion on the 2L-GeSe/*X* vdWHs

The electronic properties of gamma-GeSe are very sensitive to the number of layers, and the band gaps of 1L, 2L and 4L of  $\gamma$ -GeSe are 0.60, 0.34, and 0.04 eV, respectively. Herein, we conducted some calculations regarding the heterostructures of 2L  $\gamma$ -GeSe with the *X* layers. As shown in Table S2, the lattice constants and lattice mismatches of the fully relaxed 2L-GeSe/*X* vdWHs are slightly different from those of 1L-GeSe/*X*

vdWHs. The band structures in Fig. S9 show that the features in the band structures of 2L-GeSe and  $X$  layers are preserved, and the valence and conduction bands also show a strong hybridization between 2L-GeSe and  $X$  layers, which are in line with the trend in 1L-GeSe/ $X$  vdWHs. However, band alignments (Fig. S10) of 2L-GeSe/ $X$  vdWHs are different from that in 1L-GeSe/ $X$  vdWHs due to the bandgaps change (i.e., change in the relative positions of the valence and conduction bands) in the 2L-GeSe as well as the strain effect. In 2L-GeSe/BN vdWH, the position of the CBM of GeSe relative to BN remains unchanged (2.56 to 2.58 eV), while the VBM of GeSe is moved up, leaving a  $\Delta E_V$  to 1.65 eV. Similarly, in 2L-GeSe/Graphene vdWH, the Fermi level is located within the valence band of 2L-GeSe due to the upward shift of the VBM of GeSe, forming a metal-semiconductor ohmic contact. In 2L-GeSe/MoS<sub>2</sub> vdWH, the strain caused by the lattice mismatch makes the bandgap (1.42 eV) of MoS<sub>2</sub> smaller than that in 1L-GeSe/MoS<sub>2</sub> vdWH (1.56 eV). The change in the bandgaps of 2L-GeSe and MoS<sub>2</sub> is manifested as an up-shift of the VBM of GeSe and a down-shift of the CBM of MoS<sub>2</sub> in the 2L-GeSe/MoS<sub>2</sub> vdWH, finally forming a type-III band alignment. Therefore, the trend of interlayer interaction in 2L-GeSe/ $X$  vdWHs are basically consistent with that of 1L-GeSe/ $X$  vdWHs except for the bandgap and strain effects.

**Table S2.** The calculated lattice constants, lattice mismatches and strains of 2L- $\gamma$ -GeSe/ $X$  vdWHs.

	2L $\gamma$ -GeSe	BN	2L $\gamma$ -GeSe	Graphene	2L $\gamma$ -GeSe	MoS <sub>2</sub>
$a_0$ (Å)	3.77	2.51	3.77	2.47	3.77	3.15



$a_v$ (Å)	7.53		7.44		6.43	
$\eta$ (%)	0.13%	0	1.34%	0.40%	1.55%	2.02%
$\varepsilon$ (%)	-0.13%	0	-1.33%	+0.40%	-1.53%	+2.06%
						%

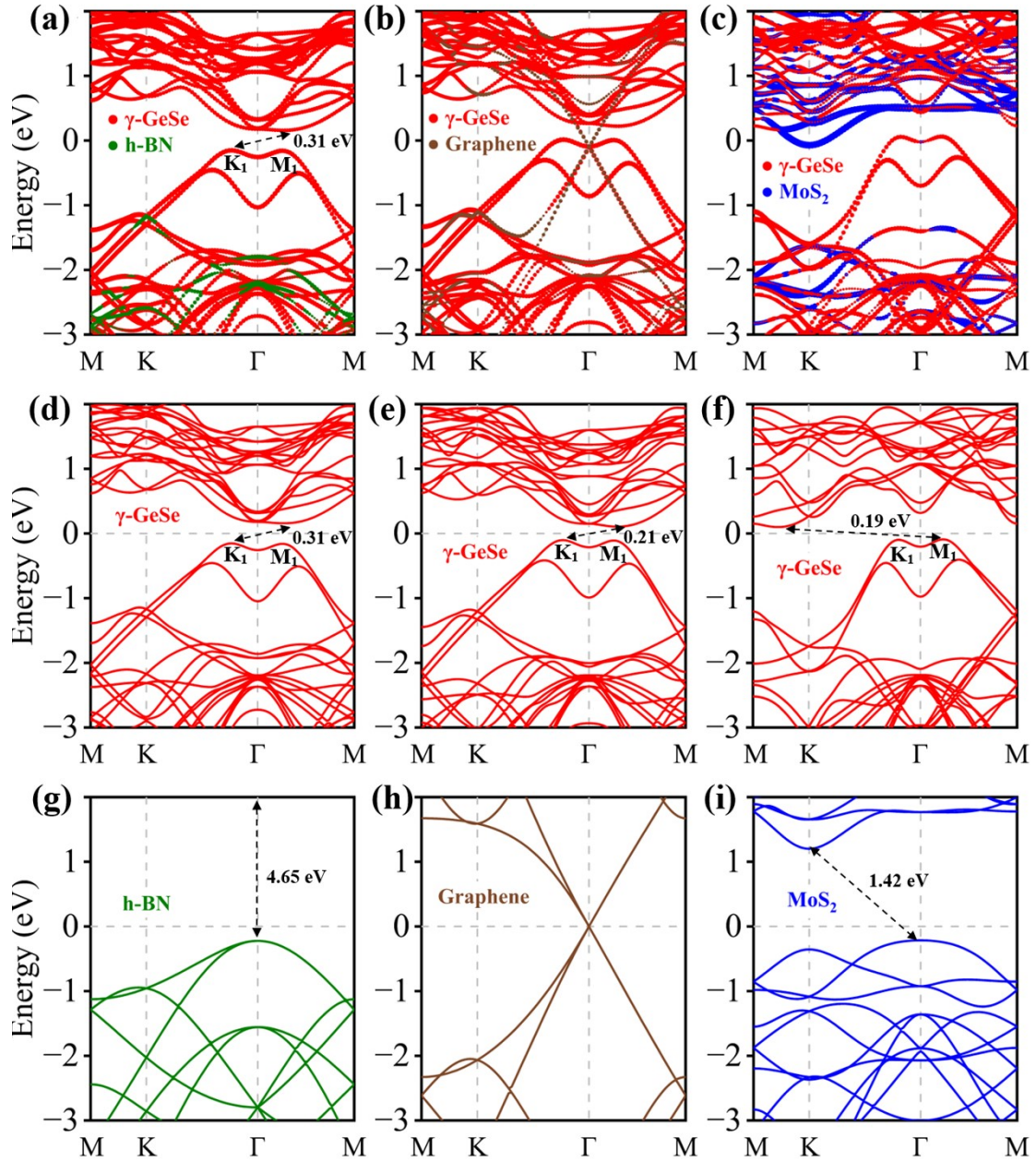


**Fig. S9** Band structures of 2L- $\gamma$ -GeSe/BN vdWH (a), and 2L- $\gamma$ -GeSe (d) and h-BN (g) monolayer under the strain equivalent to that in the 2L- $\gamma$ -GeSe/BN vdWH; band

structures of 2L- $\gamma$ -GeSe/graphene vdWH (b), and 2L- $\gamma$ -GeSe (e) and graphene (h) monolayer under the strain equivalent to that in the 2L- $\gamma$ -GeSe/graphene vdWH; band structures of 2L- $\gamma$ -GeSe/MoS<sub>2</sub> vdWH (b), and 2L- $\gamma$ -GeSe (f) and MoS<sub>2</sub> (i) monolayer under the strain equivalent to that in 2L- $\gamma$ -GeSe/MoS<sub>2</sub> vdWH.

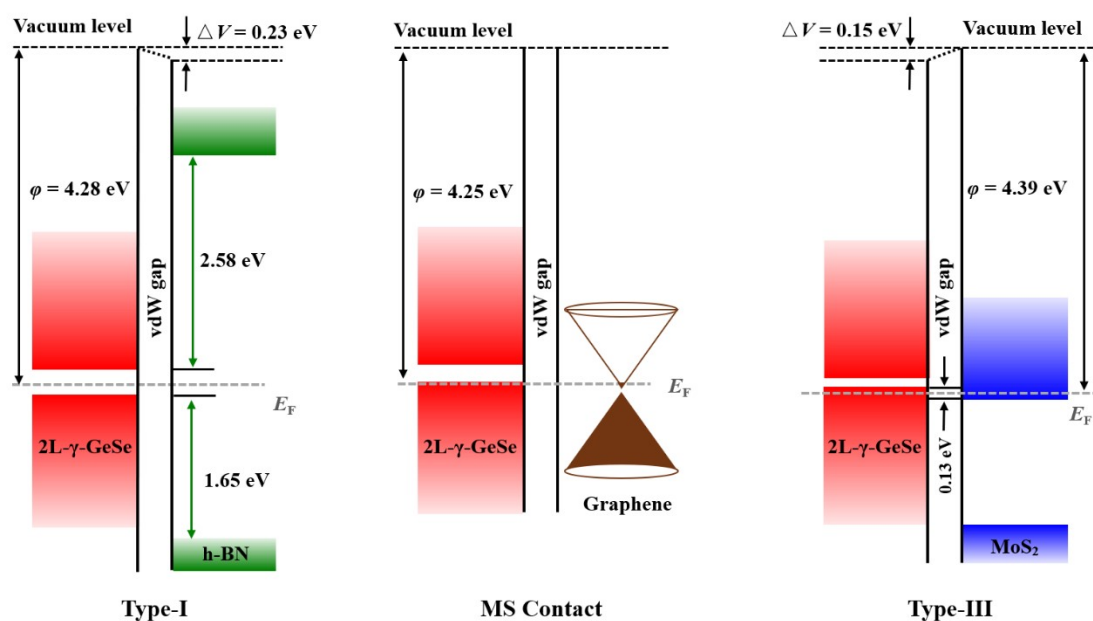


**Fig. S10** The band alignment diagrams of 2L- $\gamma$ -GeSe/BN, 2L- $\gamma$ -GeSe/graphene and 2L- $\gamma$ -GeSe/MoS<sub>2</sub> vdWHs.